Root cap cell corpse clearance limits microbial colonization in *Arabidopsis thaliana*

Nyasha M. Charura[1+], Ernesto Llamas[1+], Concetta De Quattro[1], David Vilchez[2,3,4], Moritz K. Nowack[5,6#] and Alga Zuccaro[1#*]

[1] Cluster of Excellence on Plant Sciences (CEPLAS), Institute for Plant Sciences, University of Cologne, D-50674 Cologne, Germany.

[2] Cologne Excellence Cluster for Cellular Stress Responses in Aging-Associated Diseases (CECAD), University of Cologne, 50931 Cologne, Germany.

[3] Center for Molecular Medicine Cologne (CMMC), University of Cologne, 50931 Cologne, Germany.

[4] Faculty of Medicine, University Hospital Cologne, 50931 Cologne, Germany.

[5] Department of Plant Biotechnology and Bioinformatics, Ghent University, 9052 Ghent, Belgium

[6] VIB Center for Plant Systems Biology, 9052 Ghent, Belgium

[#]shared last author

[+]shared first author

*Corresponding author: azuccaro@uni-koeln.de

Abstract

Programmed cell death occurring during plant development (dPCD) is a fundamental process integral for plant growth and reproduction. Here, we investigate the connection between developmentally controlled PCD and fungal accommodation in *Arabidopsis thaliana* roots, focusing on the root cap-specific transcription factor ANAC033/SOMBRERO (SMB) and the senescence-associated nuclease BFN1. Mutations of both dPCD regulators increase colonization by the beneficial fungus *Serendipita indica*, primarily in the differentiation zone. *smb-3* mutants additionally exhibit hypercolonization around the meristematic zone and a delay of *S. indica*-induced root-growth promotion. This demonstrates that root cap dPCD and rapid post-mortem clearance of cellular corpses represent a physical defense mechanism restricting microbial invasion of the root. Additionally, reporter lines and transcriptional analysis revealed that *BFN1* expression is downregulated during *S. indica* colonization in mature

root epidermal cells, suggesting transcriptional control as a means for microbial regulation of host dPCD.

Key findings in bullet points:

- The process of programmed cell death in root development (dPCD) influences the extent and outcomes of fungal symbiosis
- Fungal colonization of the root tip and differentiation zone is restricted by SMB-mediated clearance of dead cells, which preserves the meristem and regulates symbiosis
- The plant nuclease BFN1, which is associated with senescence, is exploited by beneficial microbes to facilitate their root accommodation

Keywords

(RCD) regulated cell death / plant-microbe interaction / growth promotion / manipulation of dPCD / SMB / meristematic stem cells / BFN1 / aging cells

Introduction

Plant roots elongate by producing new cells in the root apical meristem at the root tip. As roots extend further into the soil environment, the newly formed root tissue is naturally exposed to microbial attack, challenging the successful establishment of root systems. However, microbial colonization at the meristematic zone is rarely detected [1, 2]. The sensitive tissue of meristematic stem cells is surrounded by the root cap, a specialized root organ that orchestrates root architecture, directs root growth based on gravitropism and hydrotropism, and senses environmental stimuli. In addition, the root cap is presumed to have a protective function in soil exploration [3, 4].

In *Arabidopsis thaliana* (hereafter Arabidopsis), the root cap consists of two distinct tissues: the centrally located columella root cap at the very root tip and the peripherally located lateral root cap (LRC), which flanks both the columella and the entire root meristem [5]. A ring of specific stem cells continuously generates both new LRC cells and root epidermal cells [5]. However, despite the constant production of LRC cells, the root cap itself does not grow in size but matches the size of the meristem [3, 6, 7]. To maintain

size homeostasis, root cap development is a highly regulated process that varies in different plant species. In Arabidopsis, a combination of dPCD and shedding of old cells into the rhizosphere has been described [3, 8]. The centrally located columella root cap along with adjacent proximal LRC cells is shed as a cell package, followed by a PCD process [9, 10, 11]. In contrast, LRC cells at the distal end of the root tip elongate and reach the edge of the meristematic zone where they undergo dPCD, orchestrated as part of a terminal differentiation program by the root cap-specific transcription factor ANAC33/SOMBRERO (SMB) [6, 8, 12]. SMB belongs to a plant-specific family of transcription factors carrying a NAC domain (NAM - no apical meristem; ATAF1 and -2, and CUC2 - cup-shaped cotyledon). SMB promotes the expression of genes involved in the initiation and execution of LRC cell death, including the senescence-associated bifunctional nuclease *BFN1* and the putative aspartic protease *PASPA3* [6, 11]. BFN1 localizes in the ER, but upon cell death the protein is released and its nuclease activity ensures rapid and irreversible degradation of RNA and DNA in the nucleus and cytoplasm as part of a rapid cell-autonomous corpse clearance at the root surface [6, 13, 14]. Accordingly, DNA and RNA fragmentation in *bfn1-1* loss-of-function mutants is delayed [6]. Precise timing of cell death and elimination of LRC cells before they fully enter the elongation zone is essential for maintaining root cap size and optimal root growth [6]. Loss of SMB activity results in a delayed cell death, causing LRC cells to enter the elongation zone where they eventually die without expression of dPCD executor genes in the root cap [6]. Interestingly, the aberrant cell death of LRC cells in the elongation zone of *smb-3* mutants is not followed by corpse clearance, resulting in an accumulation of uncleared cell corpses along the entire root surface [6].

Despite its importance in root morphology and plant development, little is known about the importance of dPCD and rapid cell corpse clearance on plant-microbe interactions. To address this question, we tested two well-characterized loss-of-function T-DNA insertion lines, *smb-3* and *bfn1-1*, during colonization with *Serendipita indica*, a beneficial fungus of the order Sebacinales. As a root endophyte, *S. indica* colonizes the epidermal and cortex layers of a broad range of different plant hosts, conferring various beneficial effects, including plant growth promotion, protection against pathogenic microbes and increased tolerance to abiotic stresses [15, 16, 17]. The colonization strategy of *S. indica*

comprises an initial biotrophic interaction, followed by a growth phase associated with a restricted host cell death that does not, however, diminish the beneficial effects on the plant host. The induction of restricted cell death in the epidermal and cortex layers is a crucial component of the colonization strategy of *S. indica* and is accompanied by an increased production of fungal hydrolytic enzymes [1, 18]. The switch between biotrophic and cell death-associated phase can vary depending on the host system and environmental conditions, but has been postulated to occur approximately 6 to 8 days post inoculation (dpi) in Arabidopsis [18]. Although several effector proteins involved in fungal accommodation have been described [19, 20, 21, 22, 23, 24], the exact mechanism by which *S. indica* manipulates host cell death and the role of dPCD in fungal accommodation in the roots are largely unclear.

Here, we show that the accumulation of uncleared LRC cell corpses on the roots of *smb-3* mutants triggers hypercolonization by *S. indica*, especially around the meristematic zone, and delays *S. indica*-induced root growth promotion. We propose that a tight regulation of host dPCD and rapid and complete root cap clearance play important roles in restricting fungal colonization at the root apical meristem. Furthermore, we show that *S. indica* downregulates *BFN1* in older and differentiated epidermal cells to promote fungal accommodation. Our results emphasize that beneficial microbes have the ability to modify plant dPCD processes to enhance host colonization.

Results

The SMB-mediated clearance of dead cells protects the root meristem and regulates symbiosis

dPCD and corpse clearance are the final steps of LRC differentiation that maintain root cap organ size in root tips of Arabidopsis. This process is orchestrated by the LRC-specific transcription factor SMB and executed by its direct and indirect downstream targets (**Fig. 1A**). To characterize the role of disrupted dPCD in Arabidopsis LRCs, we analyzed the phenotypic implications of the SMB loss-of-function allele *smb-3*. We first visualized the extent of cell death in the *smb-3* T-DNA insertion line with Evans blue staining, a viability dye that penetrates non-viable and damaged/dying cells [25]. Evans blue staining highlighted the presence of uncleared LRC cell corpses along the surface of

primary roots of *smb-3* mutants, starting at the distal boarder of the meristematic zone (**Fig. 1B, C and Fig. S1A**). We further characterized *smb-3* mutants with Proteostat staining, a fluorescent dye that binds to quaternary protein structures typically found in misfolded and/or aggregated and condensed proteins (hereafter referred to as protein aggregates) [26]. Proteostat staining revealed an accumulation of protein aggregates in uncleared dead LRC cells adhering to the roots of *smb-3* mutants (**Fig. 1D – F**). Additional filter trap analysis confirmed increased levels of protein aggregates in *smb-3* mutant compared to WT roots (**Fig. 1G**). We previously observed that aggregated proteins accumulate in WT roots in dying and sloughed columella cell packages but not in young LRC-, meristematic- or healthy differentiated-cells [26]. Notably, in *smb-3* mutants, neither Proteostat nor Evans blue was detected in young LRC cells covering the meristem or in epidermal cells beneath the uncleared LRC cell corpses along the elongation and differentiation zone. This highlights that loss of SMB activity specifically affects the induction of dPCD in LRC cells at the transition between meristematic and elongation zone (**Fig. 1D, F and Fig. S1A**). These data show that the delayed cell death of LRC cells of *smb-3* mutants in the elongation zone is accompanied by an impaired protein homeostasis (proteostasis), resulting in the accumulation of misfolded and aggregated proteins in uncleared LRC cell corpses.

To assess the effects of impaired dPCD processes in the *smb-3* mutant root cap on plant-microbe interactions, we measured colonization rates of *S. indica*. We quantified extraradical colonization using the chitin-binding fluorescent marker Alexa Fluor 488 conjugated to Wheat Germ Agglutinin (WGA-AF 488) as a proxy for fungal biomass. We compared staining intensities of WGA-AF 488 between *S. indica*-colonized WT and *smb-3* roots. *S. indica* showed a clear hypercolonization phenotype along the main root axis of *smb-3* mutants (**Fig. 2A, B**). On WT roots, *S. indica* preferentially colonized the differentiation zone, leaving the meristematic and elongation zone largely uncolonized, whereas mycelial growth was clearly detectable at the root tips of *smb-3* plants (**Fig. 2A and Fig. S1B**) [1, 2]. Intraradical colonization by *S. indica* was quantified by comparing fungal and plant single-copy housekeeping marker genes using quantitative PCR (qPCR), after washing of roots to remove outer fungal mycelium. The results showed a significant increase in intraradical fungal accommodation in *smb-3* mutants compared to WT roots

(**Fig. 2C**). To assess the biological implications of hypercolonization, we measured *S. indica*-induced root growth in WT and *smb-3* mutants. While *S. indica* consistently and significantly increased root length in WT plants at 8, 10 and 14 dpi, increased length of *smb-3* mutant roots was only observable at later stages of colonization, indicating a delayed growth promotion phenotype (**Fig. 2D**). Detailed cytological analysis confirmed that *S. indica* grew extensively around the meristematic zone of *smb-3* mutants but not of WT roots (**Fig. 3A, B**) and showed increased colonization of *smb-3* mutants in the differentiation zone (**Fig. 3C**). We further observed that *S. indica* was accommodated in cells that were subject to cell death and protein aggregation in the *smb-3* background (**Fig. 3B, D, E**). Together, these findings indicate that loss of SMB activity in the root cap results in an accumulation of uncleared LRC cell corpses that promotes fungal colonization from the meristematic to the differentiation zone. Therefore, we postulate that the continuous clearance of root cap cells in WT roots is important to limit microbial colonization along the entire root axis and prevent microbial colonization in the meristematic zone.

Interestingly, Evans blue cell death staining of *S. indica*-inoculated *smb-3* mutants displayed a clearing of LRC cell corpses from the surface of *smb-3* mutant roots over time, while mock-treated *smb-3* mutant roots remained littered with LRC cell corpses (**Fig. 3F and Fig. S1C**). This observation indicates that *S. indica* is able to degrade uncleared cell corpses, which likely provide additional nutrients that fuel fungal hypercolonization in the *smb-3* mutant background.

The senescence associated plant nuclease BFN1 is exploited by beneficial microbes to facilitate root accommodation

To further explore the role of root dPCD during *S. indica* accommodation in Arabidopsis, we performed transcriptome analysis, tracking developmental cell death-marker gene expression during different colonization stages [27]. The major regulator in LRCs, *SMB*, showed no significant changes in expression during fungal colonization (**Fig**. **4A, C**). However, a marked decrease in the expression of *BFN1* was observed at 6 dpi in Arabidopsis (**Fig. 4B, C**). To validate the RNA-Seq analysis, we performed whole-root

qPCR of WT mock- and colonized-roots, confirming *BFN1* downregulation at the onset of cell death in *S. indica*-colonized plants (**Fig. 4D**).

While *SMB* expression is restricted to the LRC, *BFN1* exhibits a broader expression pattern across various cell types and tissues, such as root cap cells, cells adjacent to emerging lateral root primordia, differentiating xylem tracheary elements, as well as senescent leaves, and abscission zones of flowers and seeds [28, 29]. This widespread expression establishes BFN1 as a key player in the general regulation of dPCD and senescence processes in various tissues in Arabidopsis. To visualize the extent of *BFN1* downregulation upon *S. indica* colonization in different zones of the root, we used a transgenic *BFN1* promoter-reporter line (*pBFN1::NLS-tdTOMATO*) [11]. In agreement with the previously described GUS reporter lines [28], we detected activation of the *BFN1* promoter via accumulation of the fluorescent tdTOMATO signal in the nucleus of root cap and xylem cells in mock-treated roots (**Fig. S2A**). Additionally, we observed promoter activation in epidermal root cells of the differentiation zone (**Fig. 4E**). In the distal region of the differentiation zone in young epidermal cells, the tdTOMATO signal was observed in nuclei, while in the basal region of the differentiation zone in older epidermal cells, the tdTOMATO signal appeared to be dispersed (**Fig S2**). These findings indicate ongoing nuclear membrane degradation and cell death in the older part of the root, independent of fungal colonization and suggest activation of *BFN1* during root epidermal cell aging/senescence. Next, we inoculated the *pBFN1* reporter lines with *S. indica* and observed a reduction in promoter activity in epidermal cells that were in contact with the fungus compared with mock-treated roots (**Fig. 4E, F**). *BFN1* expression and nuclear localization in the root cap or xylem was not affected by *S. indica* colonization (**Fig. S2B**). This indicates that the downregulation of *BFN1* by *S. indica* occurs mainly in epidermal cells of the differentiation zone and is regulated independently of SMB and its activity in the root cap.

To assess the phenotypic effects of *BFN1* downregulation, we analyzed Arabidopsis *bfn1-1* KO mutants using the cell death and protein aggregates markers, Evans blue and Proteostat. Staining of *bfn1-1* mutants with Evans blue showed an increase of cell remnants in the epidermal cell layer of the differentiation zone (**Fig. 5A, B**), consistent

with a proposed delay of dPCD and cell corpse clearance by the BFN1 activity. Furthermore, while WT roots were devoid of protein aggregates, *bfn1-1* mutants exhibited aggregates along the primary root axis, starting at the transition between elongation and differentiation zone. The meristematic zone remained free of protein aggregates (**Fig. 5C, D**). These data suggest that the lack of BFN1 activity in the root cap, xylem, and senescent epidermis creates a general cellular stress in the roots that affects proteostasis in the differentiation zone (**Fig. S3**). Similar to *bfn1-1*, WT roots colonized by *S. indica* showed increased Evans blue and Proteostat signal in the differentiation zone. Aggregated proteins were detected in colonized and adjacent non-colonized cells along the differentiation zone, suggesting a non-cell autonomous host response to the fungus (**Fig. S4**).

To investigate the biological relevance of *BFN1* downregulation during *S. indica* root colonization, we quantified extraradical fungal growth using the WGA-AF 488 stain. When comparing staining intensities of *S. indica*-inoculated *bfn1-1* mutants and WT seedlings, we observed a significantly stronger fluorescence signal at the roots of *bfn1-1* mutants, indicating a higher extraradical fungal colonization along the differentiation zone (**Fig. 5E, F and Fig. S3D**). However, similar to WT roots, *bfn1-1* mutants did not exhibit fungal colonization around the meristematic zone as observed in *smb-3*-colonized roots (**Fig. 5E**). Quantification of intraradical colonization by qPCR, after removal of outer fungal mycelium, showed a significant increase of *S. indica* biomass in *bfn1-1* mutants at later stages of interaction (**Fig. 5G**). Together, these results emphasize that downregulation of *BFN1* during colonization is beneficial for intra- and extraradical fungal accommodation in the differentiation zone.

Next, we investigated the impact of other beneficial microbes on dPCD by examining transcriptional responses in Arabidopsis roots colonized by different organisms. These included *S. vermifera*, an orchid mycorrhizal fungus closely related to *S. indica*, and two bacterial synthetic communities derived from either Arabidopsis roots or the rhizosphere of *Hordeum vulgare* [16]. In all three interactions, *BFN1* expression was consistently decreased in Arabidopsis roots (**Fig. S5A**). Additionally, RNA-Seq analysis of Arabidopsis dPCD marker genes during *S. vermifera* colonization confirmed the downregulation of

BFN1 (**Fig. S5 B, C**). Our findings indicate that microbes may benefit from delayed post-mortem corpse clearance after dPCD in host plants and suggest that beneficial microbes may have evolved mechanisms to manipulate dPCD pathways to increase colonization (**Fig. 6**).

Discussion

In this study, we investigated the functional link between dPCD and microbial accommodation in roots. Impaired dPCD in the Arabidopsis *smb-3* and *bfn1-1* mutants increased colonization by the beneficial endophyte *S. indica*. The *smb-3* mutants display hypercolonization along the entire primary root, suggesting that the extra sheet of cell corpses surrounding *smb-3* roots provide additional and easily accessible nutrients that fuel fungal colonization. In fact, we observed a clearing effect with progressive colonization stages. Furthermore, hypercolonization of Arabidopsis, caused by the loss of dPCD in the root cap, mitigates the beneficial effects of *S. indica* by delaying the induction of growth promotion. Most notably, we observed hypercolonization of the meristematic zone of *smb-3* mutants (**Fig. 6**). The root apical meristem embedded in this zone of the root tip is essential for root growth, as all primary root tissue originates from these continuously dividing and differentiating stem cells [30]. This sensitive tissue is surrounded by the root cap, which protects it from external stresses [31]. The phenotype of *smb-3* mutants shows resemblance to the human skin disease hyperkeratosis. In healthy human skin, a pool of stem cells produces layers of cells that divide, differentiate, die, and are shed. Such developmental programs form a physical and dynamic barrier against environmental factors. Microbes attempting to establish themselves are consistently removed by skin exfoliation [32]. Patients with hyperkeratosis show an accumulation of dead cells on the outer skin layer, making them more susceptible to microbial infection [33]. Likewise, malfunctions within regulated cell death in mammal gut epithelial cells produce death-induced nutrient release (DINNR) that can fuel bacterial growth and infection and could cause a variety of disorders such as inflammatory diseases [34]. The importance of an intact root cap in plant-microbe interactions is further highlighter by the fact that the physical removal of root caps in maize plants leads to increased colonization of the root tip by the plant growth promoting rhizobacterium (PGPR) *Pseudomonas fluorescens* [35]

and to changes in the rhizosphere microbiome composition along the root axis [36]. Moreover, it has been suggested that border cells released from the root cap may distract root-feeding nematodes from attacking plant roots [37]. Our results provide strong evidence that root cap size maintenance in the form of constant root cap cell turnover in Arabidopsis acts as a dynamic barrier, analogous to epidermal cell turnover in animals. It thus represents a sophisticated physical mechanism to prevent or reduce intracellular microbial colonization near the root meristematic tissue and contributes to the maintenance of a beneficial interaction with root endophytes.

Mutation of *BFN1* displayed significantly increased colonization in the differentiation zone but not in the meristematic zone (**Fig. 6**). The differences in colonization patterns to the *smb-3* mutants likely reflect spatial expression and localization patterns of SMB and BFN1 activity throughout Arabidopsis roots. While the expression of the transcription factor *SMB* is restricted to the LRC, the senescence-associated nuclease *BFN1* is expressed in different tissues undergoing dPCD and senescence below and above ground [28, 29]. Here, we show that *BFN1* is additionally expressed in differentiated root epidermal cells that undergo nuclear degradation during root maturation. This suggests an age-dependent dPCD in the outer epidermal layer of Arabidopsis roots where expression of *BFN1* possibly pre-dates cortical and epidermal abscission during secondary root growth and contributes to clearance of cell corpses during periderm emergence [38]. This process resembles root cortex senescence (RCS) and cell death (RCD) in grass species such as wheat, barley, and corn, which typically start in the epidermis and spread toward the endodermis [39].

Additionally, we observe differences in the presence and distribution of protein aggregates in *smb-3* and *bfn1-1* mutants. In *smb-3* mutants protein aggregates are restricted to LRC cells adhering to the primary root. In contrast, *bfn1-1* mutation results in scattered cell death in the epidermal cell layer, which is additionally littered with protein aggregates along the differentiation zone, regardless of the occurrence of cell death.

While we show that dPCD protect the meristem from microbial colonization, we propose that some adapted microbes manipulate host dPCD processes by affecting the transcriptional expression of *BFN1* to facilitate accommodation in the root. Whether active

interference by fungal effector proteins, fungal-derived signaling molecules or a systemic response of Arabidopsis roots underlies *BFN1* downregulation by *S. indica* remains to be investigated. It was recently demonstrated that small active metabolites produced either by Toll/interleukin-1 receptor (TIR)-containing leucine-rich repeat (NLR) receptors [40] or by fungal-derived enzymes [19] through hydrolysis of RNA/DNA can mediate host cell death. This raise the exiting possibility that RNAse and DNAse activities of BFN1 may be involved in the production of small active nucleotide-derived metabolites that affect cell death, cell corpse clearance, proteostasis and fungal accommodation in the differentiation zone. This hypothesis should be followed up by metabolomic and proteomic approaches. Notably, we have shown that other beneficial microbes such as the closely related fungus *S. vermifera* and synthetic bacterial communities isolated from Arabidopsis and *H. vulgare* [16] also downregulate *BFN1* in Arabidopsis. These findings emphasize the presence of a conserved pathway influenced by diverse beneficial microbes to downregulate *BFN1* expression in epidermal tissue to facilitate symbioses.

In conclusion, our data show that tight regulation of host dPCD in epidermal- and root cap-tissue plays an important role in restricting fungal colonization. From a microbial perspective, dPCD pathways represent a potential intersection for promoting symbiotic interactions and possibly nutrient availability (**Fig. 6**). These results shed light on the complex relationship between PCD and microbial accommodation in plant roots, offering valuable insights into the development of plants that establish more efficient partnerships with beneficial microbes.

Materials and methods

Fungal strains and growth conditions

Fungal experiments were performed with *Serendipita indica* strain DSM11827 (German Collection of Microorganisms and Cell Cultures, Braunschweig, Germany). *S. indica* was grown on complete medium (CM) containing 2% (w/v) glucose and 1.5% (w/v) agar (Hilbert et al., 2012). Fungal material was grown at 28°C in the dark for 4 weeks before spore preparation. For additional experiments, *S. vermifera* (MAFF305830) was used and grown on MYP medium containing 1.5% agar at 28°C in darkness for 3 weeks before mycelium preparation for root inoculation.

Plant material and growth conditions

Seeds of *Arabidopsis thaliana* wild-type (WT) ecotype Columbia 0 (Col-0) and T-DNA insertion mutants (*bfn1-1* [GK-197G12] and *smb-3* [SALK_143526C]) in Col-0 background were used for experiments. Seeds were surface sterilized in 70% ethanol for 15 min and 100% ethanol for 12 min, stratified at 4°C in the dark for 3 days and germinated and grown on ½ MS medium (Murashige-Skoog Medium, with vitamins, pH 5.7) containing 1% (w/v) sucrose and 0.4% (w/v) Gelrite under short-day conditions (8 h light, 16 h dark) with 130 µmol $m^{-2\ s-1}$ light and 22°C/18 °C.

Fungal inoculation

One-week-old seedlings were transferred to 1/10 PNM (Plant minimal Nutrition Medium, pH 5.7) plates without sucrose, using 15 to 20 seedlings per plate. Under sterile conditions, spores of *S. indica* were scraped from agar CM plates using 0.002% Tween water (Roth), washed two times with ddH_2O and pipetted in a volume of 2 ml on plant roots and surrounding area in a concentration of $5x10^5$ spores per plate. ddH_2O was used for inoculation of mock plants. For *S. vermifera* inoculation, mycelium was scrapped from plates in ddH_2O, washed and added to Arabidopsis roots in a volume of 1 ml of a stock solution of 1 g / 50 ml.

In case of experiments using seeds inoculation with *S. indica*, Arabidopsis seeds were surface sterilized, incubated with fungal spore solution at $5x10^5$ concentration for 1 hour and plated on ½ MS plates (without sucrose).

Evans blue staining

For the visualization of cell death in Arabidopsis roots a modified protocol by [25] was used. Roots were washed three times in ddH_2O to remove lose external fungal mycelium and then stained for 15 min in 2 mM Evans blue (Sigma-Aldrich) dissolved in 0.1 M $CaCl_2$ pH 5.6. Following, roots were washed extensively with ddH_2O for 1 hour and a Leica M165 FC microscope was used for imaging. To quantify Evans blue staining intensity, ImageJ was used to invert the pictures, draw out individual roots and measure and compare mean grey values.

Extraradical colonization assays

To quantify extraradical colonization of *S. indica* on Arabidopsis, seed-inoculated plants were grown for 10 days. Inoculated and mock-treated seedlings were stained directly on plate by pipetting 2 ml of 1X PBS solution containing Alexa Fluor 488 (5 ul/mL) conjugated with Wheat Germ Agglutinin (WGA-AF 488, Invitrogen). After 2 min of incubation, the roots were washed twice on the plate with 1X PBS solution. The stained seedlings were transferred to a fresh ½ MS square plate. In order to perform a correct and focused scan of the plate with the roots, it was checked that the solid MS medium was flat and even and had no unevenness. To scan the plate, we used an Odyssey M Imaging System (LI-COR Biosciences) and the LI-COR Acquisition Software 1.1 (LI-COR Biosciences). In the software, we selected custom assay and then membrane. We selected the area in the plate to be scanned and selected the channels 488 (for WGA-Alexa Flour 488) and RGB trans (for bright field). We defined the focus offset between 3.5 mm and 4.0 mm (depending on the thickness of the MS medium). For resolution we selected 10 µm when scanning two plants or 100 µm when scanning several plants. Quantification of WGA-AF 488 fluorescence was performed using EmpiriaStudio Software (LI-COR Biosciences).

RNA extraction (intraradical colonization assay)

To measure intraradical colonization via RNA extraction and PCR, plants were harvested at three time points around 7, 10 and 14 dpi. The roots were extensively washed with ddH_2O and tissue paper was used to carefully wipe off mycelium on the surface of the roots. After cleaning the roots were shock frozen in liquid nitrogen and RNA was extracted with TRIzol (Invitrogen, Thermo Fisher Scientific, Schwerte, Germany). After a DNase I (Thermo Fisher Scientific) treatment according to the manufacturer's instructions to remove DNA, RNA was used to generate cDNA through the utilization of the Fermentas First Strand cDNA Synthesis Kit (Thermo Fisher Scientific).

Quantitative RT-PCR analysis

The quantitative real time-PCR (qRT-PCR) was performed using a CFX connect real time system (BioRad) with the following program: 95 °C 3min, 95 °C 15s, 59 °C 20s, 72 °C 30

s, 40 cycles and melting curve analysis. Relative expression was calculated using the $2^{-\Delta\Delta CT}$ method (Livak and Schmittgen 2001). qRT-PCR primers can be found in Table S1.

Filter trap analysis

Filter trap assays were performed as previously described [26, 41]. Protein extracts were obtained using native lysis buffer (300 mM NaCl, 100 mM HEPES pH 7.4, 2 mM EDTA, 2% Triton X-100) supplemented with 1x plant protease inhibitor (Merck). Cell debris was removed by several centrifugation steps at 8,000 x *g* for 10 min at 4 °C. The supernatant was separated, and protein concentration determined using the Pierce BCA Protein Assay Kit (Thermo Fisher). A cellulose acetate membrane filter (GE Healthcare Life Sciences) and 3 filter papers (BioRad, 1620161) were immersed in 1x PBS and placed in a slot blot apparatus (Bio-Rad) connected to a vacuum system. The membrane was equilibrated by 3 washes with equilibration buffer (native buffer containing 0.5% SDS). 300, 200 and 100 µg of the protein extract were mixed with SDS at a final concentration of 0.5% and filtered through the membrane. The membrane was then washed with 0.2% SDS and blocked with 3% BSA in TBST for 30 minutes, followed by 3 washes with TBST. Incubation was performed with anti-polyQ [1:1000] (Merck, MAB1574). The membrane was washed 3 times for 5 min and incubated with secondary antibodies in TBST 3% BSA for 30 min. The membrane was developed using the Odyssey M Imaging System (LI-COR Biosciences). Extracts were also analyzed by SDS-PAGE and western blotting against anti-Actin [1:5000] (Agrisera, AS132640) to determine loading controls.

Confocal laser scanning microscopy (CLSM) and Proteostat staining quantification

CLSM images were acquired using either the FV1000 confocal laser scanning microscope (Olympus) or a Meta 710 confocal microscope with laser ablation 266 nm (Zeiss). All images were acquired using the same parameters between experiments. Excitation of WGA-AF 488 was done with an argon laser at 488 nm and the emitted light was detected with a hybrid detector at 500-550 nm. Proteostat was excited at 561 nm and the signal was detected between 590-700 nm. Hoechst was excited with a diode laser at 405 nm and the emitted light was detected with a hybrid detector at 415-460 nm.

Proteostat staining

For the detection of aggregated proteins, we used the Proteostat Aggresome detection kit (Enzo Life Sciences). Seedlings were stained according to the manufacturer's instructions. Seedlings were incubated with permeabilizing solution (0.5% Triton X-100, 3 mM EDTA, pH 8.0) for 30 minutes at 4ºC with gentle shaking. The seedlings were washed twice with 1X PBS. Then the plants were incubated in the dark with 1x PBS supplemented with 0.5 µl/ml Proteostat and 0.5 µl/ml Hoechst 33342 (nuclear stain) for 30 min at room temperature. Finally, the seedlings were washed twice with 1x PBS and mounted on a slide for CLSM analysis or in mounted in fresh MS plates for LI-COR analysis. Quantification of Proteostat fluorescence was performed using Fiji software or EmpiriaStudio Software (LI-COR Biosciences).

Transcriptomic analysis

Arabidopsis Col-0 WT roots were inoculated with *S. indica*. Arabidopsis roots were harvested from mock-treated plants and inoculated plants at four different time points post inoculation: 1, 3, 6 and 10 dpi. Three biological replicates were used for each condition. The RNA-seq libraries were generated and sequenced at US Department of Energy Joint Genome Institute (JGI) under a project proposal (Proposal ID: 505829) [42, 43]. For each sample, stranded RNA-Seq libraries were generated and quantified by qRT-PCR. RNA-Seq libraries were sequenced with Illumina sequencer. Raw reads were filtered and trimmed using the JGI QC pipeline. Filtered reads from each library were aligned to the Arabidopsis genome (TAIR10) using HISAT2 [44] and the reads mapped to each gene were counted using featureCounts [45]. Samples harvested at 1 dpi were omitted from the analysis because we decided to focus on the time points at which the interaction between Arabidopsis and *S. indica* is well established. Differential gene expression analysis was performed using the R package DESeq2 [46]. Genes with an FDR adjusted p-value < 0.05 were considered as differentially expressed genes (DEGs).

Acknowledgements

We thank the imaging facilities of CECAD (A. Schauss and C. Jüngst) and CEPLAS (P.S. Tan) for their assistance with CLSM. We thank Lisa Mahdi for conducting the experiments

and providing the samples used for the RNA-seq analysis. We further would like to thank Yu Zhang, Sravanthi Tejomurthula, Daniel Peterson, Vivian Ng & Igor Grigoriev and their work performed in the work proposal (10.46936/10.25585/60001292) conducted by the U.S. Department of Energy Joint Genome Institute (https://ror.org/04xm1d337), a DOE Office of Science User Facility, is supported by the Office of Science of the U.S. Department of Energy operated under Contract No. DE-AC02-05CH11231. AZ, NC and EL acknowledge support by the German Research Foundation (DFG) - Excellence Strategy of the Federal Republic of Germany - EXC-2048/1 - project ID 390686111. AZ and NC acknowledge support by the SFB-1403-414786233 and DV by the German Excellence Strategy-CECAD, EXC 2030-390661388.

Contributions

Conceptualization: NC, EL, MN, AZ; Methodology: NC, EL, CDQ; Investigation: NC, EL, CDQ, DV, MN, AZ; Visualization: NC, EL, CDQ; Project supervision: AZ; Writing original draft: NC, EL, AZ with the help of all authors.

References

1. Deshmukh S*, et al.* The root endophytic fungus Piriformospora indica requires host cell death for proliferation during mutualistic symbiosis with barley. *Proc Natl Acad Sci U S A* **103**, 18450-18457 (2006).

2. Jacobs S*, et al.* Broad-spectrum suppression of innate immunity is required for colonization of Arabidopsis roots by the fungus Piriformospora indica. *Plant Physiol* **156**, 726-740 (2011).

3. Kumpf RP, Nowack MK. The root cap: a short story of life and death. *J Exp Bot* **66**, 5651-5662 (2015).

4. Moriwaki T, Miyazawa Y, Kobayashi A, Takahashi H. Molecular mechanisms of hydrotropism in seedling roots of Arabidopsis thaliana (Brassicaceae). *Am J Bot* **100**, 25-34 (2013).

5. Dolan L*, et al.* Cellular organisation of the Arabidopsis thaliana root. *Development* **119**, 71-84 (1993).

6. Fendrych M*, et al.* Programmed cell death controlled by ANAC033/SOMBRERO determines root cap organ size in Arabidopsis. *Curr Biol* **24**, 931-940 (2014).

476
477 7. Barlow PW. The Root Cap: Cell Dynamics, Cell Differentiation and Cap Function. *Journal of Plant*
478 *Growth Regulation* **21**, 261-286 (2002).

479
480 8. Bennett T*, et al.* SOMBRERO, BEARSKIN1, and BEARSKIN2 regulate root cap maturation in
481 Arabidopsis. *Plant Cell* **22**, 640-654 (2010).

482
483 9. Shi CL*, et al.* The dynamics of root cap sloughing in Arabidopsis is regulated by peptide signalling.
484 *Nat Plants* **4**, 596-604 (2018).

485
486 10. Feng Q, De Rycke R, Dagdas Y, Nowack MK. Autophagy promotes programmed cell death and
487 corpse clearance in specific cell types of the Arabidopsis root cap. *Curr Biol* **32**, 2110-2119 e2113
488 (2022).

489
490 11. Huysmans M*, et al.* NAC Transcription Factors ANAC087 and ANAC046 Control Distinct Aspects
491 of Programmed Cell Death in the Arabidopsis Columella and Lateral Root Cap. *Plant Cell* **30**,
492 2197-2213 (2018).

493
494 12. Willemsen V*, et al.* The NAC domain transcription factors FEZ and SOMBRERO control the
495 orientation of cell division plane in Arabidopsis root stem cells. *Dev Cell* **15**, 913-922 (2008).

496
497 13. Reza SH*, et al.* Transcriptome analysis of embryonic domains in Norway spruce reveals potential
498 regulators of suspensor cell death. *PLoS One* **13**, e0192945 (2018).

499
500 14. Farage-Barhom S*, et al.* Localization of the Arabidopsis Senescence- and Cell Death-Associated
501 BFN1 Nuclease: From the ER to Fragmented Nuclei. *Molecular Plant* **4**, 1062-1073 (2011).

502
503 15. Boorboori MR, Zhang HY. The Role of Serendipita indica (Piriformospora indica) in Improving
504 Plant Resistance to Drought and Salinity Stresses. *Biology (Basel)* **11**, (2022).

505
506 16. Mahdi LK*, et al.* The fungal root endophyte Serendipita vermifera displays inter-kingdom
507 synergistic beneficial effects with the microbiota in Arabidopsis thaliana and barley. *ISME J* **16**,
508 876-889 (2022).

509
510 17. Fesel PH, Zuccaro A. Dissecting endophytic lifestyle along the parasitism/mutualism continuum
511 in Arabidopsis. *Curr Opin Microbiol* **32**, 103-112 (2016).

512
513 18. Zuccaro A*, et al.* Endophytic life strategies decoded by genome and transcriptome analyses of
514 the mutualistic root symbiont Piriformospora indica. *PLoS Pathog* **7**, e1002290 (2011).

515

516 19. Dunken N*, et al.* A fungal endophyte-generated nucleoside signal regulates host cell death and
517 promotes root colonization. *bioRxiv*, 2022.2003.2011.483938 (2022).

518

519 20. Weiss M, Waller F, Zuccaro A, Selosse MA. Sebacinales - one thousand and one interactions with
520 land plants. *New Phytol* **211**, 20-40 (2016).

521

522 21. Akum FN, Steinbrenner J, Biedenkopf D, Imani J, Kogel K-H. The Piriformospora indica effector
523 PIIN_08944 promotes the mutualistic Sebacinalean symbiosis. *Frontiers in Plant Science* **6**,
524 (2015).

525

526 22. Wawra S*, et al.* The fungal-specific β-glucan-binding lectin FGB1 alters cell-wall composition and
527 suppresses glucan-triggered immunity in plants. *Nature Communications* **7**, 13188 (2016).

528

529 23. Nostadt R*, et al.* A secreted fungal histidine- and alanine-rich protein regulates metal ion
530 homeostasis and oxidative stress. *New Phytologist* **227**, 1174-1188 (2020).

531

532 24. Nizam S*, et al.* Serendipita indica E5'NT modulates extracellular nucleotide levels in the plant
533 apoplast and affects fungal colonization. *EMBO reports* **20**, e47430 (2019).

534

535 25. Vijayaraghavareddy P, Adhinarayanreddy V, Vemanna RS, Sreeman S, Makarla U. Quantification
536 of Membrane Damage/Cell Death Using Evan's Blue Staining Technique. *Bio Protoc* **7**, e2519
537 (2017).

538

539 26. Llamas E*, et al.* The intrinsic chaperone network of Arabidopsis stem cells confers protection
540 against proteotoxic stress. *Aging Cell* **20**, e13446 (2021).

541

542 27. Olvera-Carrillo Y*, et al.* A Conserved Core of Programmed Cell Death Indicator Genes
543 Discriminates Developmentally and Environmentally Induced Programmed Cell Death in Plants.
544 *Plant Physiol* **169**, 2684-2699 (2015).

545

546 28. Farage-Barhom S, Burd S, Sonego L, Perl-Treves R, Lers A. Expression analysis of the BFN1
547 nuclease gene promoter during senescence, abscission, and programmed cell death-related
548 processes. *J Exp Bot* **59**, 3247-3258 (2008).

549

550 29. Escamez S*, et al.* Cell Death in Cells Overlying Lateral Root Primordia Facilitates Organ Growth in
551 Arabidopsis. *Curr Biol* **30**, 455-464 e457 (2020).

552

553 30. Hamamoto L, Haves MC, Rost TL. The production and release of living root cap border cells is a
554 function of root apical meristem type in dicotyledonous angiosperm plants. *Ann Bot* **97**, 917-923
555 (2006).

556

557 31. Kumar N, Iyer-Pascuzzi AS. Shedding the Last Layer: Mechanisms of Root Cap Cell Release. *Plants*
558 *(Basel)* **9**, (2020).

559
560 32. Dettmer P. *Immune: The new book from Kurzgesagt - a gorgeously illustrated deep dive into the*
561 *immune system*. Hodder & Stoughton (2021).

562
563 33. Cheng J, Syder AJ, Yu QC, Letai A, Paller AS, Fuchs E. The genetic basis of epidermolytic
564 hyperkeratosis: a disorder of differentiation-specific epidermal keratin genes. *Cell* **70**, 811-819
565 (1992).

566
567 34. Anderson CJ*, et al.* Microbes exploit death-induced nutrient release by gut epithelial cells.
568 *Nature* **596**, 262-267 (2021).

569
570 35. Humphris SN*, et al.* Root cap influences root colonisation by Pseudomonas fluorescens SBW25
571 on maize. *FEMS Microbiol Ecol* **54**, 123-130 (2005).

572
573 36. Ruger L*, et al.* Root cap is an important determinant of rhizosphere microbiome assembly. *New*
574 *Phytol* **239**, 1434-1448 (2023).

575
576 37. Rodger S, Bengough AG, Griffiths BS, Stubbs V, Young IM. Does the Presence of Detached Root
577 Border Cells of Zea mays Alter the Activity of the Pathogenic Nematode Meloidogyne incognita?
578 *Phytopathology* **93**, 1111-1114 (2003).

579
580 38. Wunderling A*, et al.* A molecular framework to study periderm formation in Arabidopsis. *New*
581 *Phytol* **219**, 216-229 (2018).

582
583 39. Drew MC, He CJ, Morgan PW. Programmed cell death and aerenchyma formation in roots.
584 *Trends Plant Sci* **5**, 123-127 (2000).

585
586 40. Yu D*, et al.* TIR domains of plant immune receptors are 2',3'-cAMP/cGMP synthetases mediating
587 cell death. *Cell* **185**, 2370-2386 e2318 (2022).

588
589 41. Llamas E*, et al.* In planta expression of human polyQ-expanded huntingtin fragment reveals
590 mechanisms to prevent disease-related protein aggregation. *Nature Aging*, (2023).

591
592 42. Zuccaro A, Langen G. Host-specific regulation of effector gene expression in mutualistic root
593 endophytic fungi (Proposal ID: 505829). (ed^(eds). JGI Award (2020).

594
595 43. Eichfeld R*, et al.* Time-resolved transcriptomics reveal a mechanism of host niche defense:
596 beneficial root endophytes deploy a host-protective antimicrobial GH18-CBM5 chitinase.
597 *bioRxiv*, 2023.2012.2029.572992 (2023).

598
599 44. Kim D, Langmead B, Salzberg SL. HISAT: a fast spliced aligner with low memory requirements.
600 *Nat Methods* **12**, 357-360 (2015).

601
602 45. Liao Y, Smyth GK, Shi W. featureCounts: an efficient general purpose program for assigning
603 sequence reads to genomic features. *Bioinformatics* **30**, 923-930 (2014).

604
605 46. Love MI, Huber W, Anders S. Moderated estimation of fold change and dispersion for RNA-seq
606 data with DESeq2. *Genome Biol* **15**, 550 (2014).

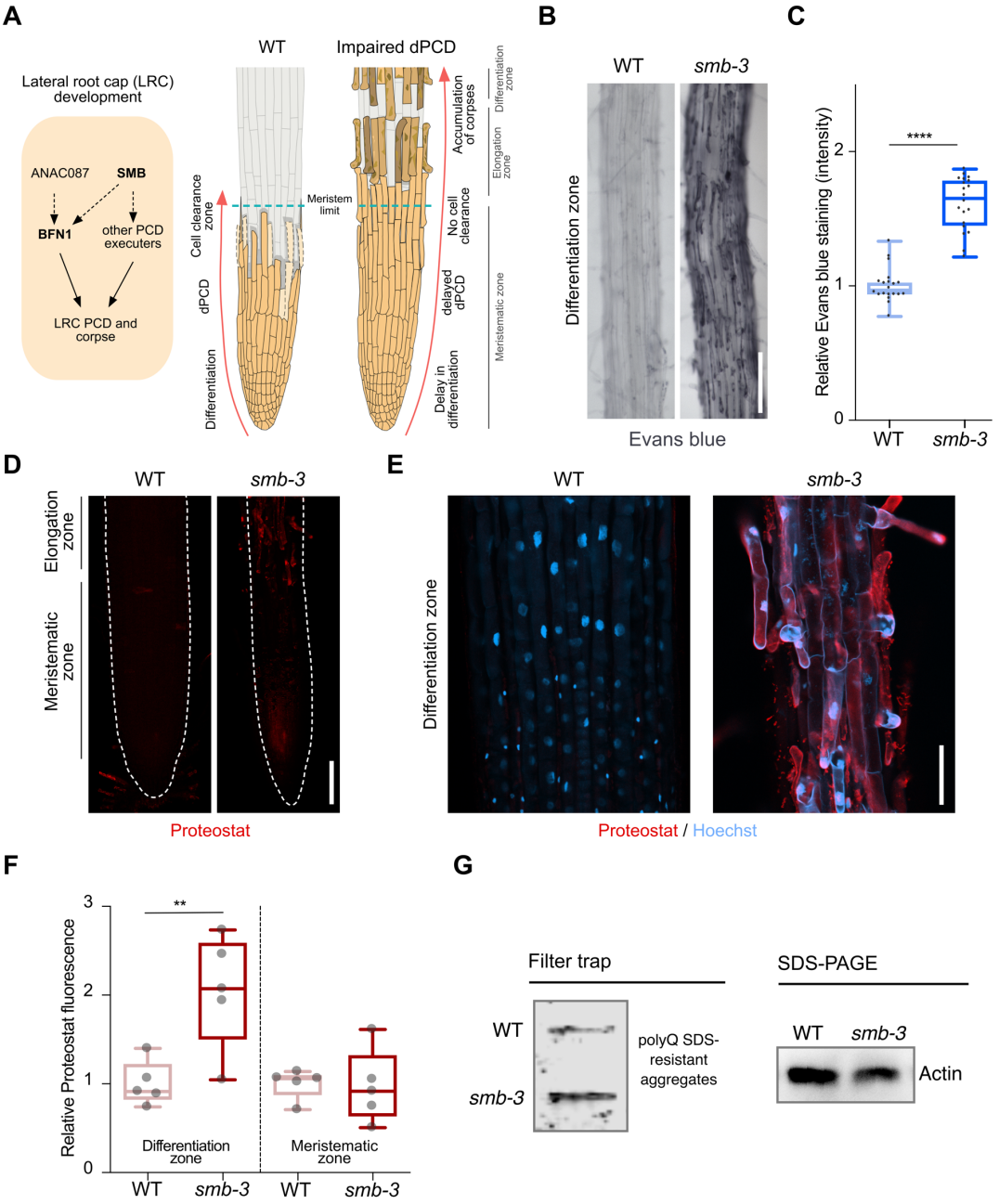

Figure 1. *smb-3* mutant roots exhibit uncleared cell corpses loaded with misfolded / aggregated proteins. (A) Schematic representation of lateral root cap (LRC) development in WT and *smb-3* mutant plants, impaired in dPCD. (B) Evans blue staining of the differentiation zone in 14-day-old WT and *smb-3* roots. Scale indicates 100 µm. (C) Relative quantification of Evans blue staining of the differentiation zone in 14-day-old WT and *smb-3* mutant roots (in reference to B). 5 plants per genotype were used, taking 4 images per plant along the main root axis. Statistical relevance was determined by unpaired, two-tailed Student's t test before normalization (****P < 0.0001). (D) CLSM images of 10-day-old WT and *smb-3* mutant roots stained with Proteostat (red) showing the meristematic- and the beginnings of the elongation-zone. Scale indicates 100 µm. (E) Magnification of the differentiation zone of WT and *smb-3* mutant roots. Proteostat (red) and Hoechst (blue) channels are shown. Scale indicates 50 µm. (F) Quantification of relative Proteostat fluorescence levels, comparing the

differentiation and meristematic zones of WT and *smb-3* mutants. 5 x 10-day-old plants were used for each genotype. Statistical significance was determined by one-way ANOVA and Tukey's post hoc test before normalization (significance threshold: P 0.05). (G) Filter trap and SDS-PAGE analysis with anti-poly-glutamine (polyQ) antibodies of 15-day-old WT and *smb-3* mutant roots. The images are representative of two independent experiments.

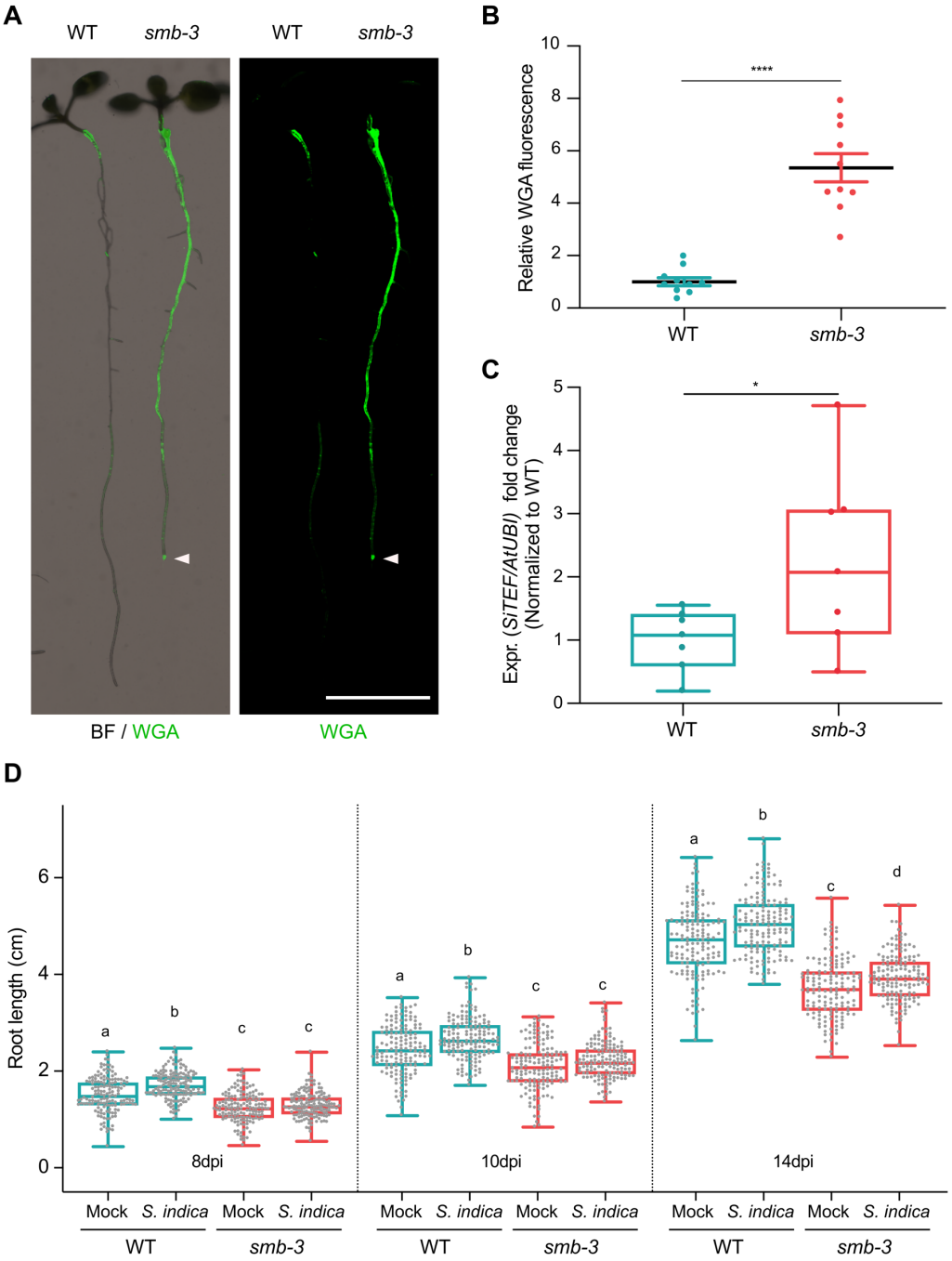

Figure 2. *smb-3* mutants display extraradical hypercolonization and increased intraradical colonization by *S. indica*. (A) Representative images show extraradical colonization of 10-day-old WT and *smb-3* mutant seedlings (seed inoculated). *S. indica* was stained with WGA-AF 488. Roots were scanned and captured with a LI-COR Odyssey M imager using the bright field (BF) and Alexa Fluor 488 channel (green). White arrowheads indicate colonization of the root tip in the *smb-3* mutant background. Scale indicates 5 mm. (B) Relative quantification of WGA-AF 488 signal as proxy for extraradical colonization on *smb-3* mutants and WT roots (in reference to A). The statistical comparison was made by two-tailed Student's t test for unpaired samples (****P < 0.0001) using 10 plants. (C) Measurement of intraradical colonization in WT and *smb-3* mutant roots were performed by qPCR. Roots from 7 biological

30 replicates were collected and washed to remove extra-radical hyphae, using approximately
31 30 seedlings for each genotype per replicate. The graph is normalized to WT for relative
32 quantification of colonization. Statistical analysis was done via two-tailed Student's t test for
33 unpaired samples (*P = 0.0466). (D) Root length measurements of WT and *smb-3* mutants,
34 with mock or *S. indica* treatments (seed inoculated) over a two-week time-period show *S.*
35 *indica*-induced growth promotion in WT roots at all time points. Growth promotion of *smb-3*
36 mutants during *S. indica* colonization was delayed and only observed at later stages of
37 colonization but not during earlier time points. To assess growth promotion, 3 biological
38 replicates for both genotypes were used, each with around 40 plants per replicate. Root
39 length was measured at 8, 10 and 14 dpi and statistical analysis was performed via one-way
40 ANOVA and Tukey's post hoc test (significance threshold: P = 0.05).

41

42

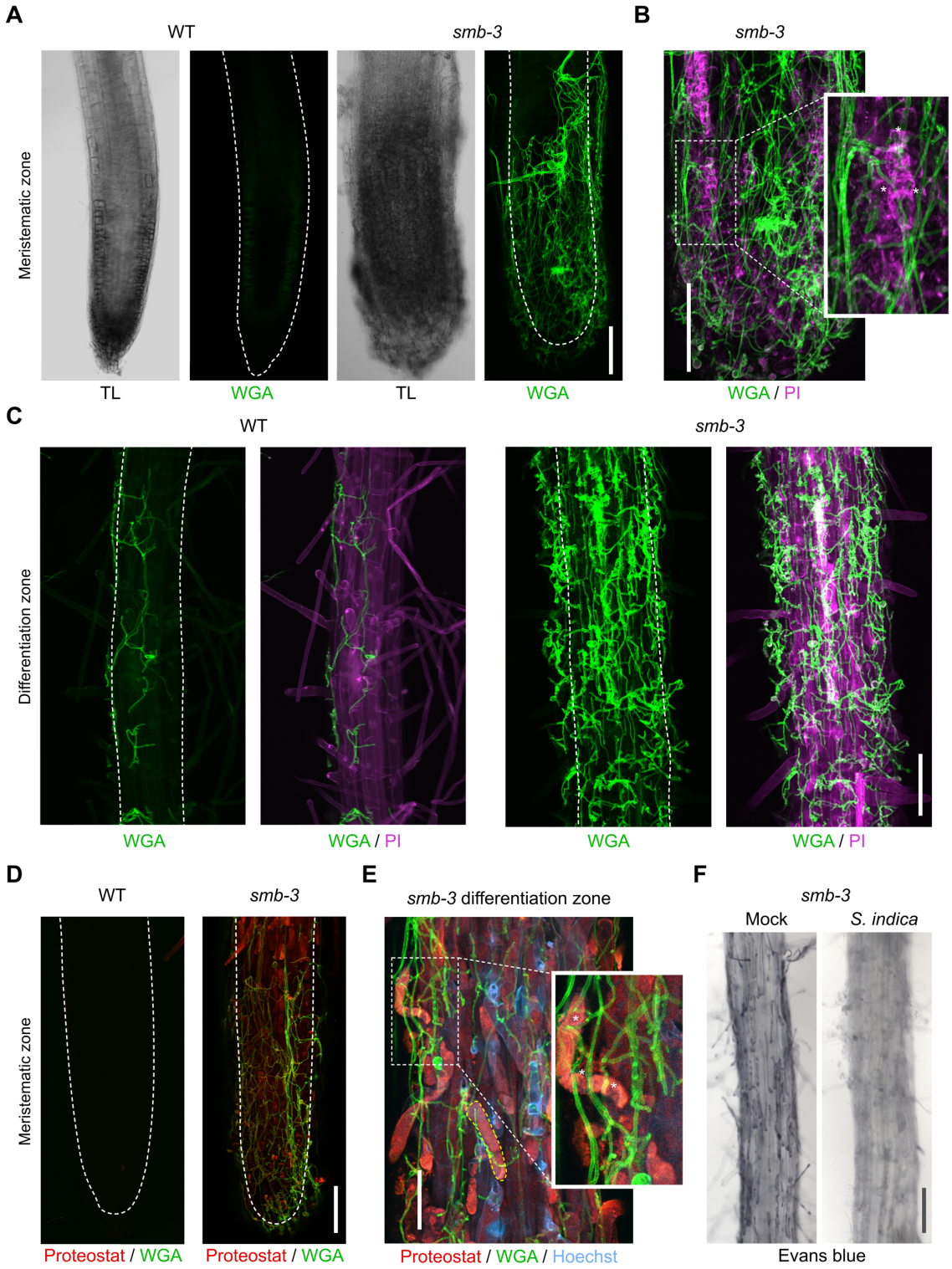

43

44 **Figure 3. Cytological analyses of *S. indica*-colonized *smb-3* mutants and WT roots.** For CLSM
45 analyses, 7-day-old seedlings were inoculated with *S. indica* spores and roots were analyzed
46 at 10 dpi. (A) Representative images of the meristematic zone of Arabidopsis WT and *smb-3*
47 mutants during *S. indica* colonization. WGA-AF 488 stain (green) was used to visualize fungal
48 structures. Transmitted light (TL) images are also shown. Scale indicates 100 µm (B)
49 Magnification of a *smb-3* mutant root tip colonized with *S. indica*. Asterisks indicate
50 penetration of hyphae into dead cells stained with propidium iodide (PI – magenta). Scale

indicates 100 µm. (C) Representative images of the differentiation zone of WT and *smb-3* mutants colonized with *S. indica* and stained with WGA-AF 488 and PI. Scale indicates 100 µm. (D) Representative images of the meristematic zone of WT and *smb-3* mutant root tips inoculated with *S. indica*, stained with WGA-AF 488 and Proteostat (red). Scale indicates 100 µm (E) Magnification of the root differentiation zone of *smb-3* mutants showing *S. indica* colonization, stained with WGA-AF 488, Hoechst and Proteostat. Penetration of fungal hyphae into uncleared cell corpses is marked with asterisks. Dotted yellow line indicates LRC cell corpse. Scale indicates 50 µm. (F) Representative images of the differentiation zone of *S. indica*-colonized WT and *smb-3* roots at 10 dpi, stained with Evans blue. Scale indicates 100 µm.

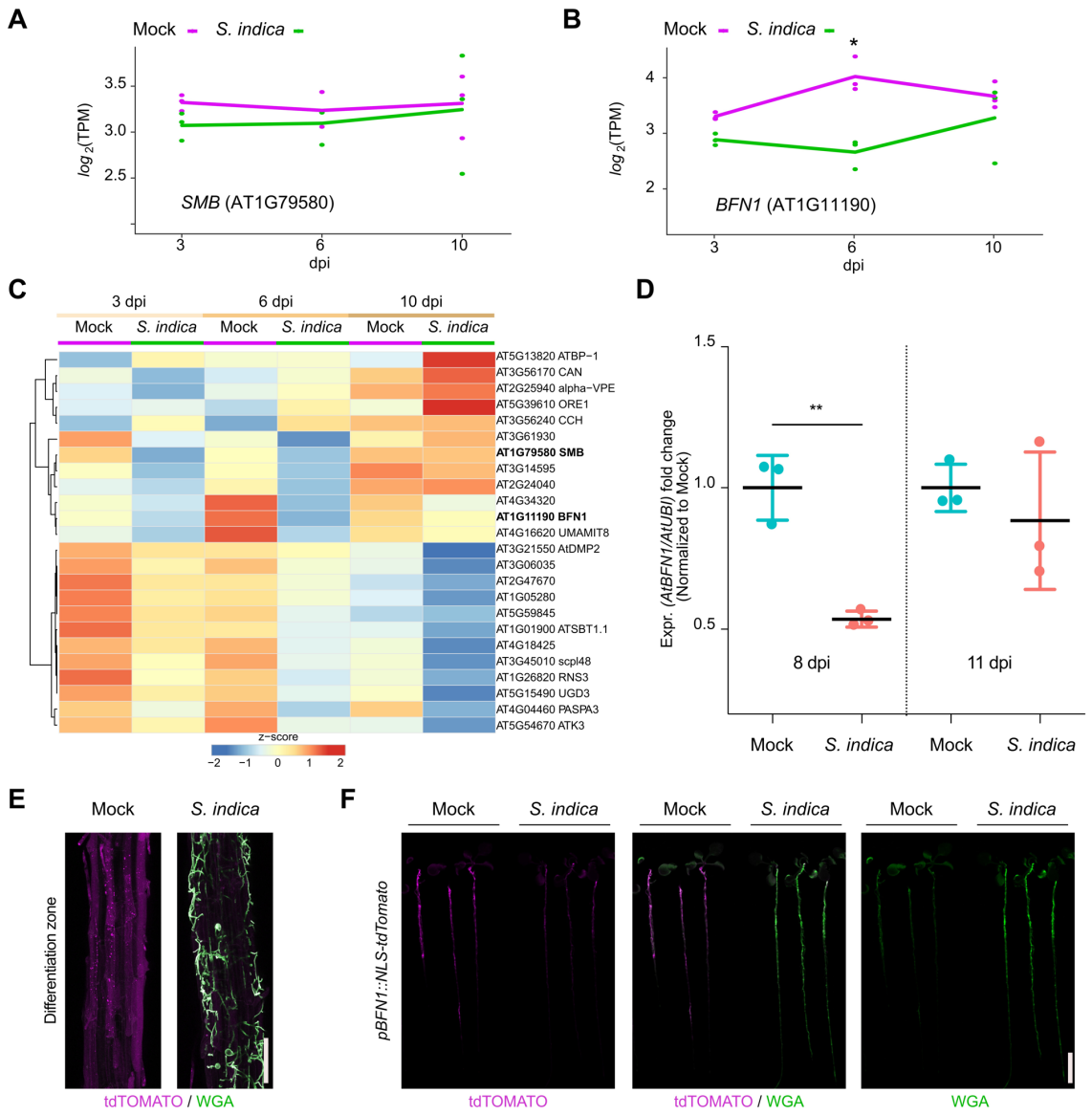

Figure 4. *BFN1* is downregulated during interaction with *S. indica*. RNA-Seq expression profiles of (A) *SMB* and (B) *BFN1* in Arabidopsis roots mock-treated or inoculated with *S. indica* at 3, 6 and 10 dpi. The log2-transformed TPM values are shown and the lines indicate average expression values among the 3 biological replicates. Asterisk indicates significantly different expression (adjusted p-value < 0.05) (C) The heat map shows the expression values (TPM) of Arabidopsis dPCD marker genes with at least an average of 1 TPM across Arabidopsis roots mock-treated or inoculated with *S. indica* at 3, 6 and 10 dpi. The TPM expression values are log2 transformed and row-scaled. Genes are clustered using spearman correlation as distance measure. Each treatment displays the average of three biological replicates. The dPCD gene markers were previously defined (Olvera-Carrillo et al., 2015). (D) *BFN1* expression in WT Arabidopsis during *S. indica* colonization at 8 and 11 dpi. RNA was isolated from 3 biological replicates for qPCR analysis, comparing *BFN1* expression with an Arabidopsis ubiquitin marker gene. (E) Representative CLSM images of the differentiation zone of mock- and *S. indica*-colonized *pBFN1::NLS-tdTOMATO* reporter roots at 7dpi. The tdTOMATO signal (magenta)

77 represents BFN1 expression and *S. indica* was stained with WGA-AF 488 (green). Scale
78 indicates 100µm. (F) Whole seedling scans of mock- and *S. indica*-treated *pBFN1::NLS-*
79 *tdTOMATO* plants taken with a LI-COR Odyssey M imager at 7dpi. Images show *BFN1*
80 expression via tdTOMATO signal alone, BFN1 expression together with *S. indica* stained by
81 WGA-AF 488 and *S. indica* colonization alone. Scale indicates 5mm.

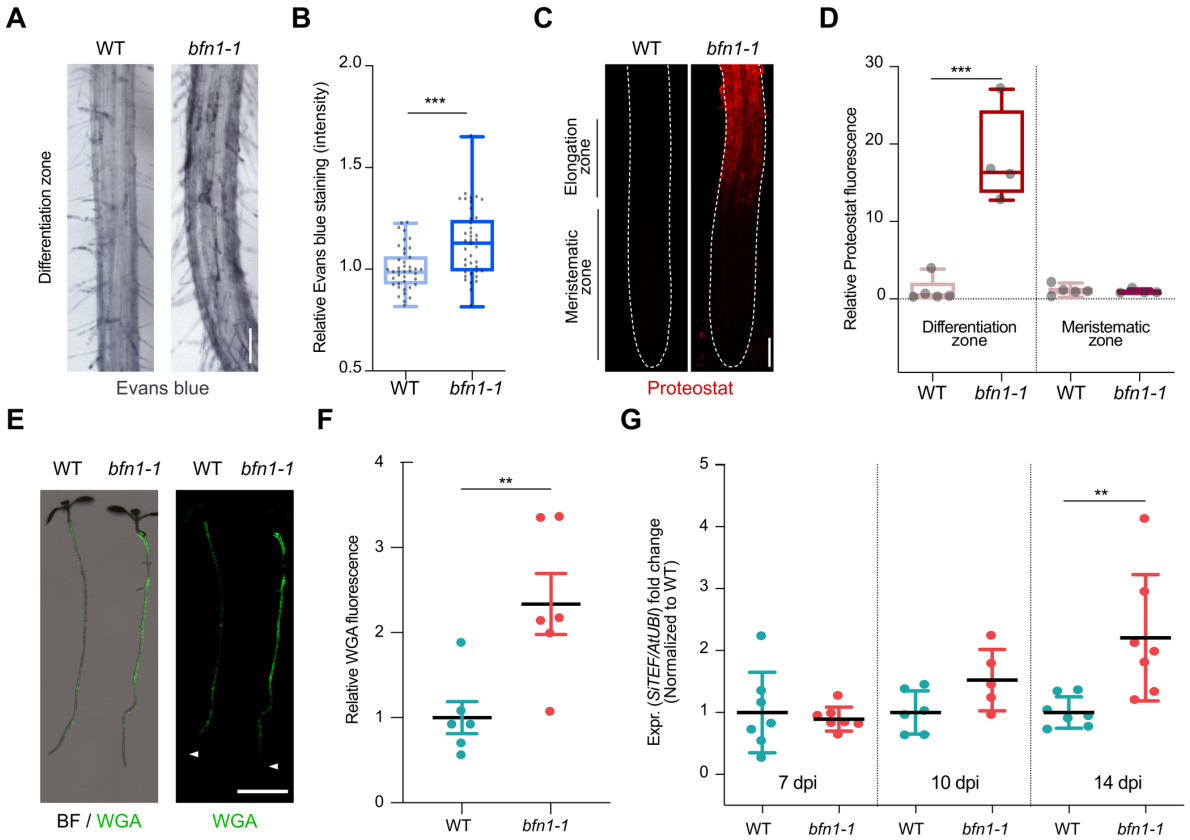

Figure 5. *BFN1* downregulation promotes fungal accommodation. (A) Microscopy images of the differentiation zone of 14-day-old WT and *bfn1-1* mutant roots, stained with Evans blue. Scale indicates 100 µm. (B) Quantification of Evans blue staining (in reference to A), comparing 14-day-old WT and *bfn1-1* mutants. 10 plants were used for each genotype, taking 4 pictures along the main root axis per plant. ImageJ was used to calculate the mean grey value to compare relative staining intensity. Statistical significance was determined using an unpaired, two-tailed Student's t test before normalization (*** $P < 0.0001$). (C) Proteostat staining of 10-day-old WT and *bfn1-1* mutant root tips. Scale indicates 100 µm. (D) Quantification of Proteostat staining (in reference to C) using 4 to 5 10-day-old WT and *bfn1-1* mutants. Statistical analysis was performed via one-way ANOVA and Tukey's post hoc test before normalization (significance threshold: $P \leq 0.05$). (E) Extraradical colonization of 10-day-old WT and *bfn1-1* mutant plants, seed-inoculated with *S. indica* and stained with WGA-AF 488 (green). Roots were scanned and captured with a LI-COR Odyssey M imager. Arrowheads indicate the position of the uncolonized root tips. Scale indicates 5 mm. (F) Relative quantification of extraradical colonization of *bfn1-1* mutant and WT roots, using WGA-AF 488 signal as a proxy for fungal biomass (in reference to E). Statistical comparisons were made by unpaired, two-tailed Student's t test for unpaired samples (**$P < 0.01$) (G) Intraradical colonization of WT and *bfn1-1* mutants was measured via qPCR. Roots from 7 biological replicates were collected and washed to remove outer extraradical mycelium, using approximately 30 plants per time point and replicate for each genotype. Each time point was normalized to WT for relative quantification of colonization. Statistical analysis was performed via one-way ANOVA and Tukey's post hoc test (significance threshold: P 0.05).

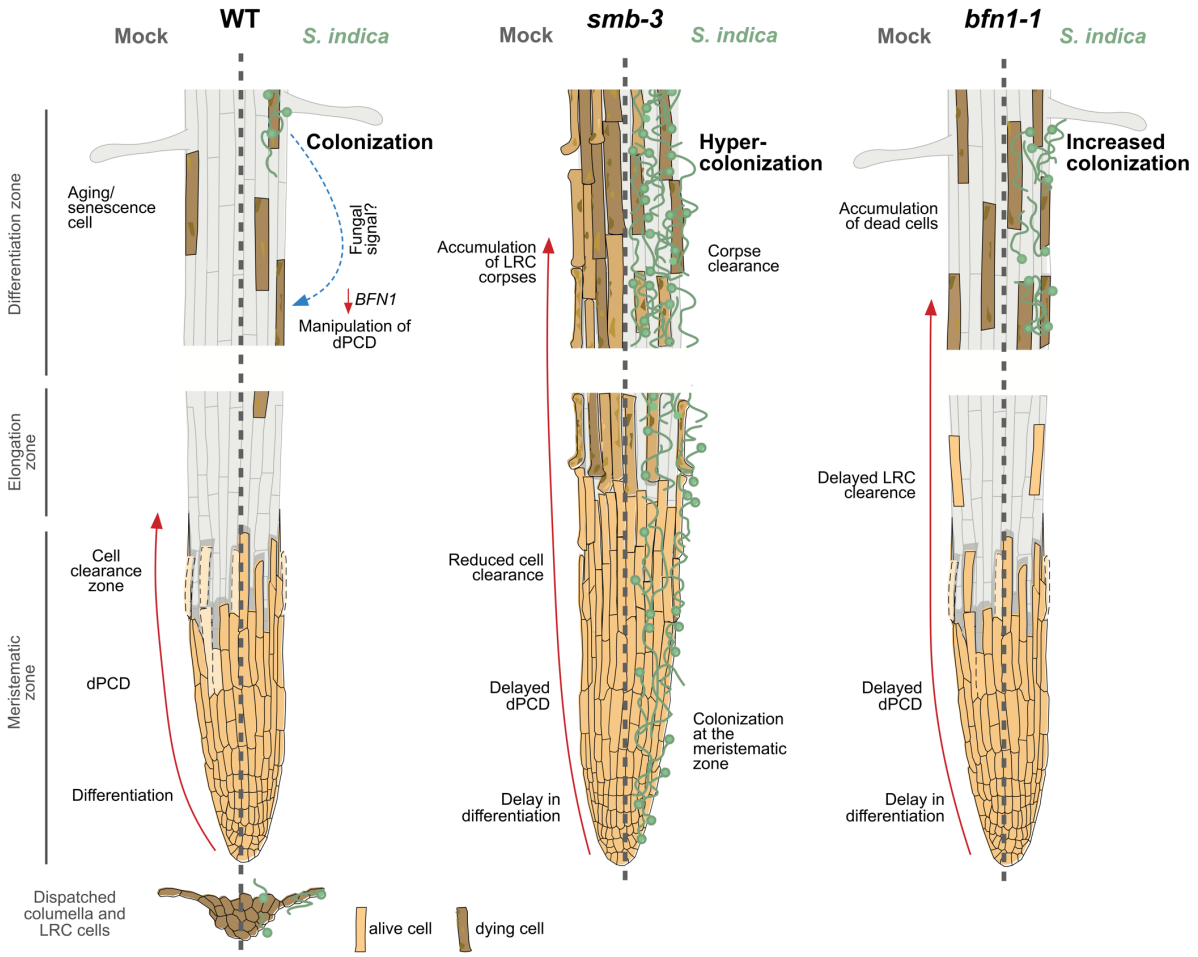

Figure 6. dPCD and its proposed effects on plant-microbe interactions. The root cap protects and covers the stem cells of the root apical meristem. Its size in Arabidopsis is maintained by a high cellular turnover of root cap cells. While the columella root cap is shed from the root tip, a dPCD machinery marks the final step of LRC differentiation and prevents LRC cells from entering into the elongation zone. Induction of cell death by the transcription factor SMB is followed by irreversible DNA fragmentation and cell corpse clearance, mediated by the nuclease BFN1, a downstream executor of dPCD (Fendrych et al., 2014). The absence of dPCD induction in the *smb-3* knockout mutant leads to a delay in LRC differentiation and allows LRC cells to enter the elongation zone, where they die uncontrolled, resulting in an accumulation of LRC cell corpses along the differentiation zone. In a WT background, the fungal endophyte *S. indica* colonizes the differentiation zone of Arabidopsis roots and can also be found in shed columella cell packages. The impaired dPCD of the *smb-3* mutant phenotype results in a hypercolonization of Arabidopsis, along the differentiation zone as well as the meristematic zone, highlighting that the continuous clearance of root cap cells is necessary for restricting microbial accommodation at the meristematic zone. Loss of the downstream dPCD executor *BFN1* does not affect fungal colonization in the meristematic zone but increases accommodation by *S. indica* in the differentiation zone, where BFN1 appears to be involved in dPCD of senescent epidermal cells and undergoes downregulation during *S. indica* colonization.